Journal of Chemical Crystallography (2025) 55:216–222
https://doi.org/10.1007/s10870-025-01051-8

ORIGINAL PAPER

Crystal Structure of Methyl 2,3-di-*O*-benzyl-α-D-(4-^{2}H)-Glucopyranoside

Hani Mobarak[1] · Vadim Kessler[2] · Lars Eriksson[1] · Göran Widmalm[1]

Received: 22 January 2025 / Accepted: 23 April 2025 / Published online: 14 May 2025

Abstract
Methyl 2,3-di-*O*-benzyl-α-D-(4-^{2}H)-glucopyranoside, $C_{21}H_{25}DO_6$, is an intermediate used in synthesis of oligosaccharides. The hexopyranose ring has the $^4C_1$ chair conformation in the crystal structure. The exocyclic groups of the hexose sugar show for the glycosidic torsion angle ϕ=−52.8° and for the hydroxymethyl group the *gauche-gauche* conformation with ω = −64.7°, one of the two main orientations of the latter group in hexopyranose sugars that have the *gluco*-configuration, i.e., with an equatorial hydroxyl group at C4. The benzene rings of the benzyl groups are arranged with an angle of 56.9° to each other within the molecule and show intramolecular as well as intermolecular C-H⋯π interactions. A chain of intermolecular hydrogen bonds exists along the b-axis involving O4 and O6 atoms. The experimentally observed peak in the infrared spectrum at 2159 cm^{-1} was ascribed to the stretching of the C4–D4 bond based on DFT calculations.

Graphical Abstract
In the structure of the monosaccharide methyl 2,3-di-*O*-benzyl-α-D-(4-^{2}H)-glucopyranoside, $C_{21}H_{25}DO_6$, the two hydroxyl groups HO4 and HO6 act as both donors and acceptors resulting in an intermolecular hydrogen bond chain along the b-axis direction.

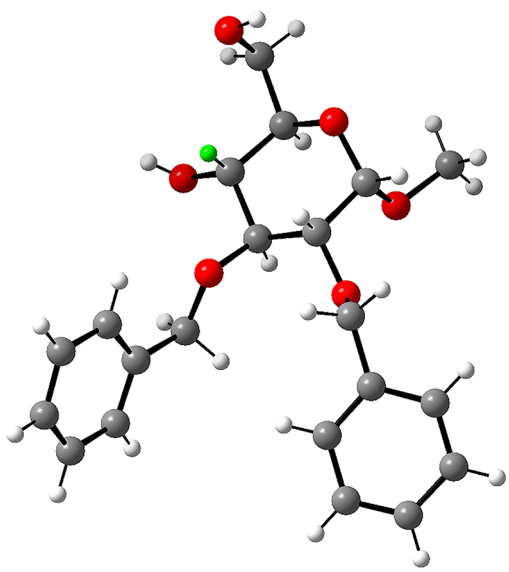

Keywords Crystal structure · Carbohydrate · Deuteration · Hydrogen bonding · Infrared

✉ Göran Widmalm
goran.widmalm@su.se

[1] Department of Chemistry, Stockholm University, Stockholm SE-106 91, Sweden

[2] Department of Molecular Sciences, SLU, Box 7015, Uppsala SE-750 07, Sweden

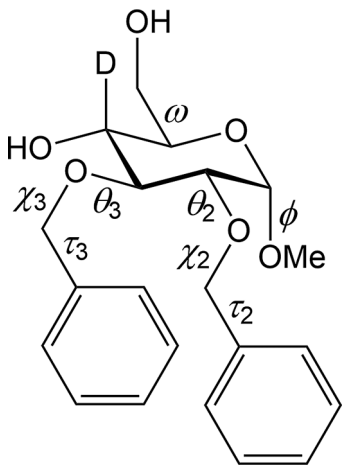

Fig. 1 Schematic representation of methyl 2,3-di-*O*-benzyl-α-D-(4-^{2}H)-glucopyranoside (I)

Table 1 Crystal data for methyl 2,3-di-*O*-benzyl-α-D-(4-^{2}H)-glucopyranoside (I)

Sum formula	$C_{21}H_{25}DO_6$
Formula Weight / g·mol^{-1}	375.42
CCDC-code	2,417,798
Temperature / K	296(2)
Wavelength / Å	0.71073 (MoKα)
Crystal size / mm	0.24 × 0.20 × 0.08
Crystal habit	plate
Crystal system	monoclinic
Space group	$P2_1$ (nr. 4)
Unit cell dimensions	a = 8.8884(8) Å b = 6.0907(5) Å c = 19.1722(17) Å β = 101.0830(10) °
Volume	1018.56(15) Å^3
Z	2
Density, ρcalc	1.224
Linear absorption coefficient	0.089 mm^{-1}
F(000)	400
Radiation source	Sealed tube
Measurement device	Bruker D8 Quest ECO
Θ_{min}, Θ_{max}	2.75, 25.7
Index ranges,	−10 ≤ h ≤ 10, −7 ≤ k ≤ 7, −23 ≤ l ≤ 23
Reflections collected	10,694
Unique reflections	3824
Observed reflections (I ≥ 2σ(I))	3080
Rint	0.0211
Parameters	248
R1a (obs data), R1 (all data)	0.0388, 0.0529
wR2b (obs data), wR2 (all data)	0.0961, 0.1044
GOOF	1.02
Residual densities (min, max, rms)	−0.122, 0.191, 0.026

[a]$R1 = \sum(||F_o|-|F_c||)/\sum(|F_o|)$, [b]$wR2 = (\sum w(F_o^2-F_c^2)^2/\sum F_o^2)^{1/2}$

Introduction

Carbohydrates play many important roles in biological systems [1] and synthesis of oligosaccharides and glycoconjugates facilitates the investigation of structure in relation to function. Synthesized oligosaccharides with well-defined structures, i.e., without heterogeneity that may be present in samples of biological origin, are essential in studies of carbohydrate-protein interactions [2, 3], for carbohydrate-based vaccines [4–6] and in glycan microarray applications [7, 8].

The all-hydrogen isotopologue of the title compound has been used in synthesis of oligosaccharides [9–14].The monodeuterated isotopologue of the title compound (Fig. 1) was used in the synthesis of a site-specifically deuterium-substituted cellobiose derivative [15], since this facilitated a detailed conformational analysis to be carried out on the disaccharide [16].

Experimental

Synthesis and Crystallization

Methyl 2,3-di-*O*-benzyl-α-D-(4-^{2}H)-glucopyranoside was synthesized according to a literature procedure [15, 17]. The obtained colorless syrup was dissolved in a minimal amount of 2-propanol and an excess of *n*-pentane was added. The solution was left at 4 °C overnight to obtain the product as a tuft of colorless needles.

Single Crystal Diffraction

The crystals of the title compound where mounted with epoxy glue on a thin glass fiber and mounted on a Bruker platform equipped with an APEX-II detector. Several ω scans were done at different φ in order to collect reflections inside the Ewald sphere. The crystal to detector distance was 40 mm. Data reduction was done with the APEX-II software package (Bruker AXS Inc., Madison, Wisconsin, USA). A summary of the crystallographic data is found in Table 1.

Structure Solution and Refinement

The structure was solved by direct methods using SHELXS [18] and refined using full matrix least square calculations using SHELXL-2019/3 [19] with anisotropic displacement parameter on all non-hydrogen atoms. Most of the non-hydrogen atoms were located in the initial electron density map and the rest of them in subsequent difference Fourier maps. All hydrogen atoms were geometrically placed and allowed to ride on the carbon or oxygen atom to which they were connected and refined with a riding model available in SHELXL. The hydroxyl hydrogens were allowed to rotate

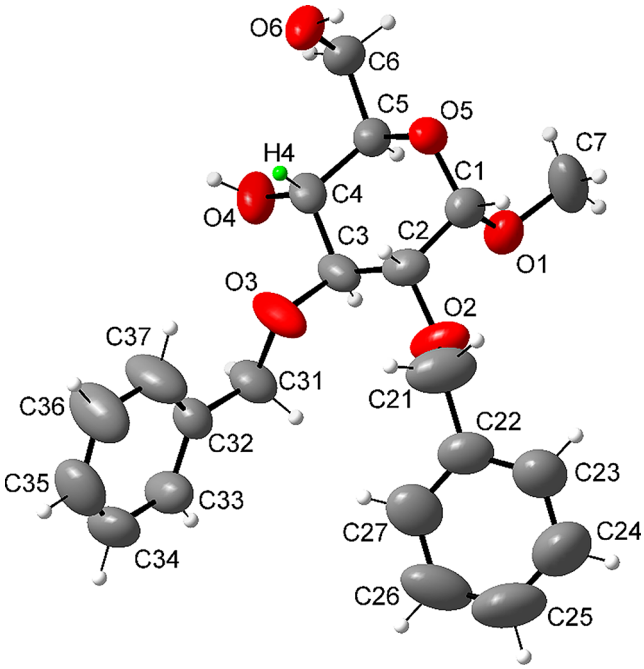

Fig. 2 Methyl 2,3-di-*O*-benzyl-α-D-(4-^{2}H)-glucopyranoside (I) with atomic labels. Anisotropic displacement ellipsoids drawn at 50% probability level

Table 2 Selected torsion angles in monosaccharide I. Standard uncertainties are not given for those containing calculated positions of hydrogen atoms

Torsion angle	Defined by atoms	X-ray value (°)	DFT value (°)
ϕ	H1-C1-O1-C7	−52.8	−46.8
ω	O5-C5-C6-O6	−64.7(3)	−61.6
θ_2	H2-C2-O2-C21	−4.9	25.3
θ_3	H3-C3-O3-C31	−2.7	−24.9
χ_2	C2-O2-C21-C22	170.4(3)	−173.5
χ_3	C3-O3-C31-C32	178.7(3)	−177.6
τ_2	O2-C21-C22-C23	100.8(5)	20.9
τ_3	O3-C31-C32-C33	−166.1(3)	−149.1

around the corresponding cone in the direction of the C-O bond. The Flack parameter [20] was inconclusive but the absolute configuration could be assigned by reference to invariance of the configuration of the chiral center.

Infrared Spectroscopy

The infrared (IR) spectrum of the title compound (I) was acquired with a Perkin-Elmer Spectrum 100 instrument. The sample was diluted by dry KBr and pressed into a tablet. The measurements were carried out in the interval 400–4000 cm^{-1} in transmission mode.

Computational Chemistry

Geometry optimization and calculated IR spectra were obtained by DFT methods using 6-31G*/B3LYP level of theory with the software NWChem [21]. Potential energy curves were computed at the same level of theory with the torsion angles τ and/or χ constrained, whereas all other degrees of freedom were free to be optimized. The geometry optimizations and IR frequency calculations for the two isotopologues of the title compound I were done using single isolated molecules.

Results and Discussion

In the title monosaccharide (I) the glycosidic torsion angle ϕ has the *exo*-anomeric conformation and the exocyclic hydroxymethyl group has the *gauche-gauche* conformation, relating O5 to O6 and C4 to O6 (Fig. 2; Table 2). Both of these exocyclic groups populate anticipated conformational states [22]. The pyranoid ring form having six heavy atoms can be characterized by puckering parameters [23], O5 → C5, as a $^4C_1$ chair with Q=0.543(3) Å, θ=7.8(3)° and φ=356(2)°. The benzyl substituents at O2 and O3 show syn-periplanar relationships for both θ_{C2} and θ_{C3}, a finding also observed in a 4-*O*-benzyl-substituted rhamnose derivative [24]. Whereas the intramolecular dihedral angle between planes defined by the two benzene rings is 62.8(2)°, the intermolecular dihedral angle between planes defined by the two benzene rings is 56.9(2)°. An intermolecular hydrogen bond network is observed with O4···H6-O6 and O6···H4-O4 (Table 3; Fig. 3). Furthermore, the hydrophobic packing around z=0 in the ab-plane is dominated by π–π stacking (Fig. 4). The two benzyloxy groups show different geometrical orientations to the central sugar ring as shown by the dihedral angle between the plane C2-O2-C21 and the benzene ring defined by C22 up to C27, that is 83.5(2)°, while the dihedral angle between the plane defined by C3-O3-C31 and the benzene group defined by C32 up to C37 is 15.7(3)°.

At the benzyl group substituting position O3 of the sugar the torsion angle at the benzene group has an s-*trans* conformation, τ_3=−166.1°, only slightly deviating from a canonical s-*trans* conformation (Table 2). In contrast, τ_2=+100.8° having a+anticlinal conformation with O2-C21 and C22-C23 almost at a right angle to each other. In a 4-*O*-benzyl-substituted rhamnose derivative [24] the corresponding torsion angle was −124.9° whereas in a 4-*O*-benzoyl-substituted rhamnose derivative [25] the torsion angle at the benzene group was +174.1°, i.e., in the latter case hardly deviation from an ideal s-*trans* conformation. The observation that the torsion angle τ of the benzyl group may deviate to a large degree from an s-*trans* conformation whereas

Table 3 Hydrogen bonds in monosaccharide I

D	H	A	D-H (Å)	H···A (Å)	D···A (Å)	D-H···A (°)	Symmetry code (A)
O6	H6	O4	0.82	1.99	2.726(3)	148.6	x, y − 1, z
O4	H4A	O6	0.82	1.86	2.682(3)	178.0	−x + 1, y + 1/2, −z + 1

that of a benzoyl group does so only to a smaller extent or hardly at all in these crystal structures was further investigated by computation of the torsion angle potential of these two functional groups, an ether vs. and ester, specifically benzyl methyl ether vs. methyl benzoate. DFT calculations at the 6-31G*/B3LYP level of theory revealed that the torsional barrier at the torsion angle τ was only 2.1 kJ·mol^{-1} in benzyl methyl ether whereas for methyl benzoate the barrier for τ was 31.7 kJ·mol^{-1}, i.e., a difference of one order of magnitude (Fig. 5). The torsional barrier of the former is even lower than that of ethane being ~12 kJ·mol^{-1} [26] and one may conclude that deviations from an s-*trans* conformation for τ torsion angles in the solid state are the effect of intermolecular forces (crystal packing) leading to changes in conformation. For the single molecule I geometry optimized in vacuo the torsion angles θ_2 and θ_3, and τ_2 deviated the most to the solid-state structure (Table 2). In the DFT calculations on the model substances the torsional energy landscape corresponding to the τ torsion did show that the rotational barrier in the ether was indeed very small, thus explaining that different values of τ torsions easily can be obtained in the crystal structure.

As the title compound I is an isotopologue of the natural abundance compound methyl 2,3-di-*O*-benzyl-α-D-glucopyranoside one can anticipate that the vibrational frequency of the C4-D4 bond is lower than that of the C4-H4 bond, which is anticipated to have a band due to a bond stretch at ~3000 cm^{-1}. The experimental IR spectrum revealed a small peak at 2159 cm^{-1} (Fig. 6) and the computed IR frequency from the geometry optimized structure I confirmed a band in this spectral region, computed to be resonating at 2256 cm^{-1} for the C4-D4 bond, whereas for the isotopologue containing the C4-H4 bond the computed frequency was at 2961 cm^{-1}.

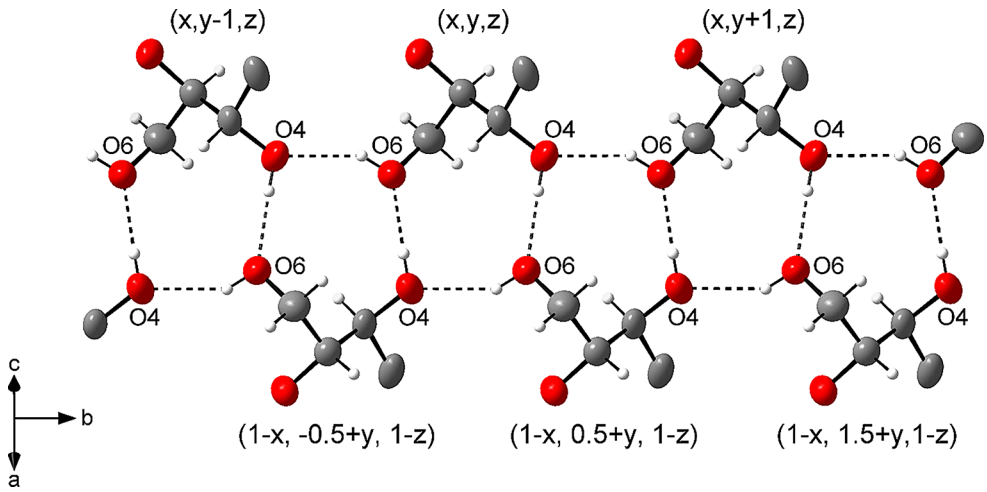

Fig. 3 Intermolecular hydrogen bonding scheme in monosaccharide (I) along the b-axis direction with codes for the symmetry equivalent units marked. Only a small part of each molecule is shown for clarity

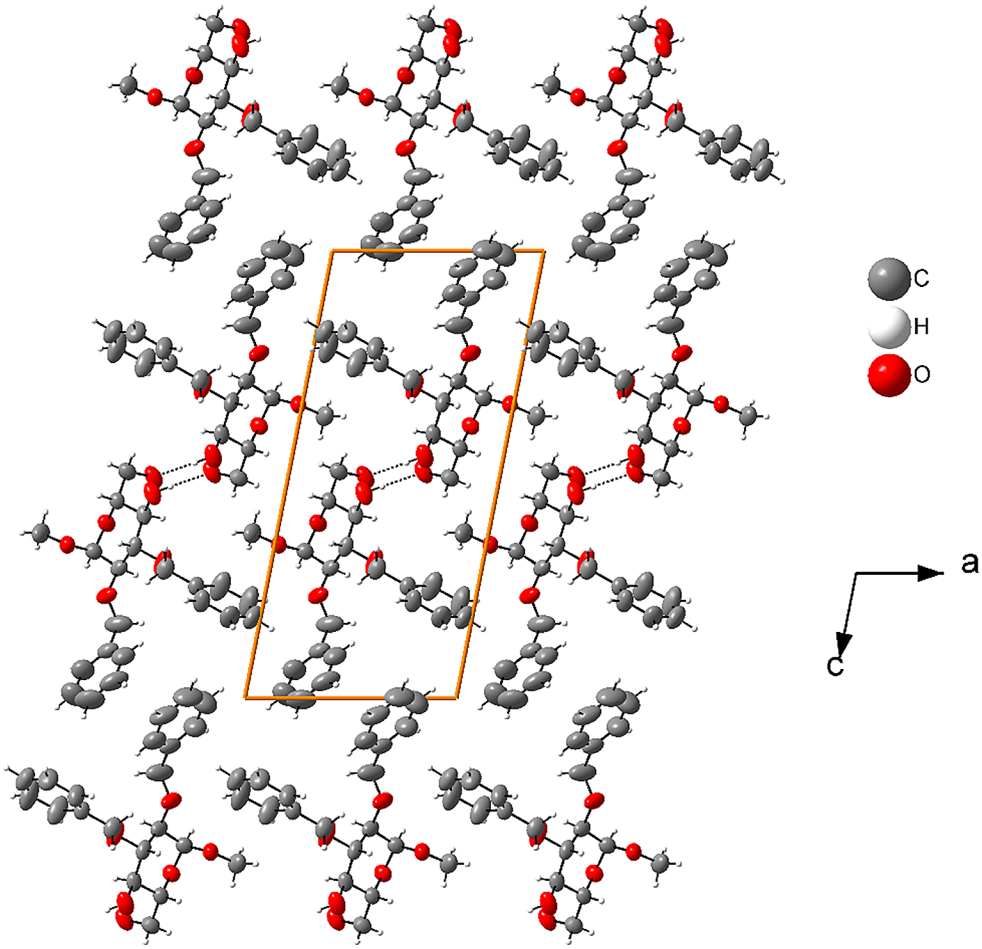

Fig. 4 Packing view along the b-axis for the crystal structure of monosaccharide I. Intermolecular hydrogen bond interactions at c = 0.5 along the b direction and hydrophobic interactions between benzene rings, at c = 0 in the ab-plane

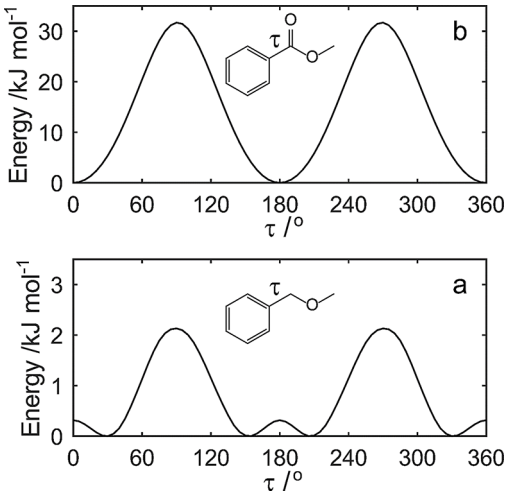

Fig. 5 Potential energy (kJ·mol^{-1}) relative to the energy minimum of the DFT geometry optimized structure vs. the τ torsional angle (C_{ortho}-C_{ipso}-C-O) constrained whereas the χ torsion angle (C_{ipso}-C-O-C_{Me}) and other degrees of freedom were free to be optimized; (**a**) benzyl methyl ether and (**b**) methyl benzoate. Note that the energy scale of the vertical axes differs by one order of magnitude

Acknowledgements The DFT computations were performed on resources provided by the Swedish National Infrastructure for Computing (SNIC) at HPC2N (UMU), Sweden, as well as on in-house workstations. This work has received financial support from the Swedish Research Council (2022-03014).

Author Contributions Hani Mobarak synthesized and crystallized the compound Vadim Kessler acquired experimental XRD and IR data and solved initial structure Lars Eriksson refined crystal structure, performed calculations of IR spectra, made figures and wrote the manuscript Göran Widmalm made figures and wrote the manuscript.

Funding Open access funding provided by Stockholm University.

Data Availability Data available within the article and from CCDC withdeposition number 2417798.

Declarations

Competing Interests The authors declare no competing interests.

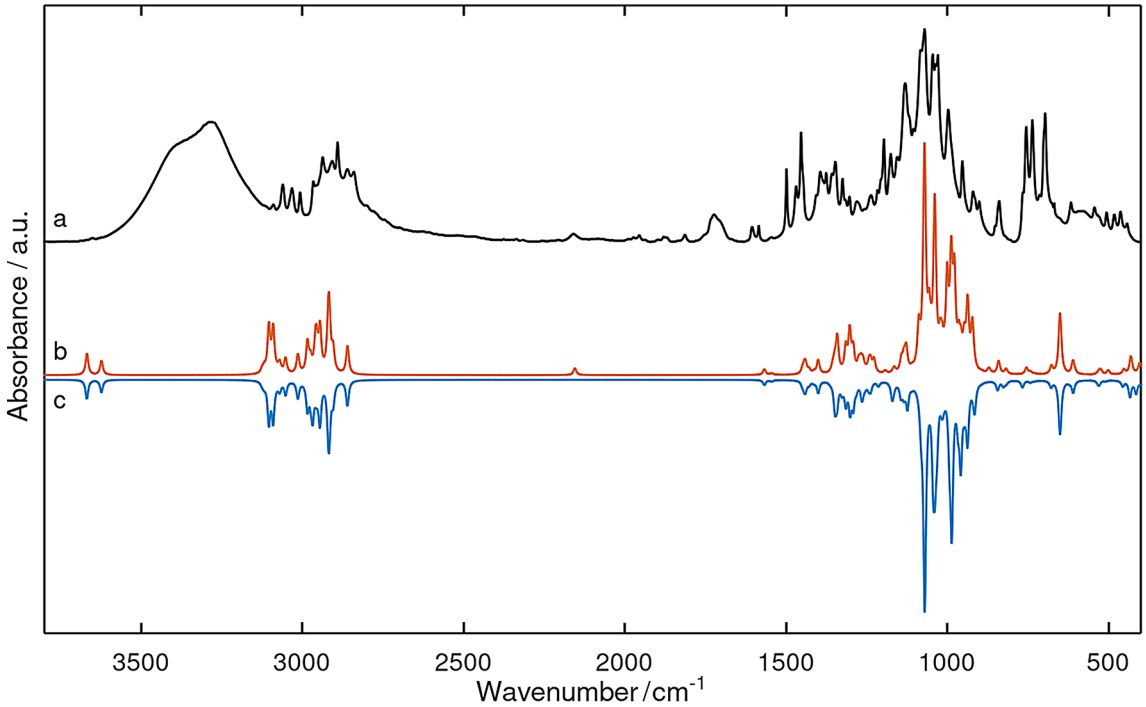

Fig. 6 IR spectra of title compound (I) obtained by measurement (**a**), while (**b**) and (**c**) were calculated using DFT with deuterium at D4 position in (**b**) and hydrogen at H4 position in (**c**). For clarity the spectrum in (**c**) has been mirrored. The observed peak for the deuterated compound at 2159 cm^{-1} can be ascribed to the stretch of C4-D4, while the corresponding computed C4-H4 stretch occurs at 2961, cm^{-1}. The two computed spectra, (**b**) and (**c**) have been shifted by 97 cm^{-1} to lower frequency to fit the position of the C4-D4 stretch in the observed spectrum

References

1. Varki A, Cummings RD, Esko JD et al (2022) Essentials of glycobiology, fourth edition. Cold Spring Harbor Laboratory Press, Cold Spring Harbor NY
2. Landström J, Nordmark E-L, Eklund R et al (2008) Interaction of a *Salmonella enteritidis* O-antigen octasaccharide with the phage P22 tailspike protein by NMR spectroscopy and Docking studies. Glycoconj J 25:137–143. https://doi.org/10.1007/s10719-007-9065-9
3. Illyés TZ, Malinovská L, Rőth E et al (2021) Synthesis of tetravalent Thio- and Selenogalactoside-Presenting galactoclusters and their interactions with bacterial lectin PA-IL from *Pseudomonas aeruginosa*. Molecules 26:542. https://doi.org/10.3390/molecules26030542
4. Mettu R, Chen C-Y, Wu C-Y (2020) Synthetic carbohydrate-based vaccines: challenges and opportunities. J Biomed Sci 27:9. https://doi.org/10.1186/s12929-019-0591-0
5. Stefanetti G, Borriello F, Richichi B et al (2022) Immunobiology of carbohydrates: implications for novel vaccine and adjuvant design against infectious diseases. Front Cell Infect Microbiol 11:808005. https://doi.org/10.3389/fcimb.2021.808005
6. van der Put RMF, Smitsman C, de Haan A et al (2022) The First-in-Human synthetic Glycan-Based conjugate vaccine candidate against *Shigella*. ACS Cent Sci 8:449–460. https://doi.org/10.1021/acscentsci.1c01479
7. Gao C, Wei M, McKitrick TR et al (2019) Glycan microarrays as chemical tools for identifying glycan recognition by immune proteins. Front Chem 7:833. https://doi.org/10.3389/fchem.2019.00833
8. Kim Y, Hyun JY, Shin I (2022) Glycan microarrays from construction to applications. Chem Soc Rev 51:8276–8299. https://doi.org/10.1039/D2CS00452F
9. Davis NJ, Flitsch SL (1994) Chemical synthesis of disaccharides which are partial structures of the glycosaminoglycan Heparan sulfate. J Chem Soc Perkin 1:359–368. https://doi.org/10.1039/p19940000359
10. Müller M, Schmidt RR (2001) Synthesis of Trisaccharides and Tetrasaccharides by Means of Intramolecular Glycosylation Supported by Rigid Spacers. European J Org Chem 2055–2066. https://doi.org/10.1002/1099-0690(200106)2001:11%3C;2055::AID-EJOC2055%3E;3.0.CO;2-N
11. Boulineau FP, Wei A (2004) Mirror-Image carbohydrates: synthesis of the unnatural enantiomer of a blood group trisaccharide. J Org Chem 69:3391–3399. https://doi.org/10.1021/jo035789l
12. Hederos M, Konradsson P (2005) Synthesis of the core tetrasaccharide of *Trypanosoma C Ruzi* glycoinositolphospholipids: man *p* (α1→6)-Man *p* (α1→4)-6-(2-aminoethylphosphonic acid)-GlcN*p*(α1→6)-*myo*-Ins-1-PO_4. J Org Chem 70:7196–7207. https://doi.org/10.1021/jo0508595
13. Tiwari P, Misra AK (2007) Synthesis of a Pentasaccharide Repeating Unit of the Extracellular Polysaccharide Produced by *Lactobacillus Delbrueckii* Subsp. *Bulgaricus* 291. J Carbohydr Chem 26:239–248. https://doi.org/10.1080/07328300701410676
14. Tiwari VK, Kumar A, Schmidt RR (2012) Disaccharide-Containing macrocycles by click chemistry and intramolecular glycosylation. Eur J Org Chem 2945–2956. https://doi.org/10.1002/ejoc.201101815
15. Söderman P, Widmalm G (1999) Stereospecific deuteration in the synthesis of Methyl α-(4-^{2}H)-cellobioside. J Org Chem 64:4199–4200. https://doi.org/10.1021/jo982256h
16. Larsson EA, Staaf M, Söderman P et al (2004) Determination of the conformational flexibility of Methyl α-Cellobioside in solution by NMR spectroscopy and molecular simulations. J Phys Chem A 108:3932–3937
17. Mobarak H, Engström O, Lahmann M, Widmalm G (2015) Stereoselective reduction using sodium triacetoxyborodeuteride: synthesis of Methyl 2,3-Di-O-benzyl-α-D-(4-^{2}H)-glucopyranoside. In: Roy R, Vidal S (eds) Carbohydrate chemistry: proven synthetic methods. CRC, Boca Raton, pp 81–87
18. Sheldrick GM (2008) A short history of SHELX. Acta Crystallogr A64:112–122. https://doi.org/10.1107/S0108767307043930
19. Sheldrick GM (2015) Crystal structure refinement with SHELXL. Acta Crystallogr C71:3–8. https://doi.org/10.1107/S2053229614024218
20. Flack HD (1983) On Enantiomorph-Polarity Estimation. Acta Cryst A39:876–881
21. Aprà E, Bylaska EJ, de Jong WA et al (2020) NWChem: past, present, and future. J Chem Phys 152:184102. https://doi.org/10.1063/5.0004997
22. Widmalm G (2013) A perspective on the primary and three-dimensional structures of carbohydrates. Carbohydr Res 378:123–132. https://doi.org/10.1016/j.carres.2013.02.005
23. Cremer D, Pople JA (1975) A general definition of ring puckering coordinates. J Am Chem Soc 97:1354–1358. https://doi.org/10.1021/ja00839a011
24. Pendrill R, Eriksson L, Widmalm G (2014) Methyl 4-O-benzyl-α-L-rhamnopyranoside. Acta Crystallogr Sect E Struct Rep Online 70:o561–o562. https://doi.org/10.1107/S1600536814007922
25. Jonsson KHM, Eriksson L, Widmalm G (2006) Methyl 4-O-benzoyl-2,3-O-isopropylidene-α-L-rhamnopyranoside. Acta Crystallogr C 62:o447–o449. https://doi.org/10.1107/S0108270106021603
26. Quijano-Quiñones RF, Quesadas-Rojas M, Cuevas G, Mena-Rejón GJ (2012) The rotational barrier in Ethane: A molecular orbital study. Molecules 17:4661–4671. https://doi.org/10.3390/molecules17044661